

## Performance of a Submerged Wave Focusing Structure in a Current

Kwok Fai Cheung

Department of Ocean Engineering, University of Hawaii at Manoa, Honolulu, HI, U.S.A.

Joong Woo Lee

Department of Ocean Civil Engineering, Korea Maritime University, Pusan, Korea

### ABSTRACT

A time-domain numerical model is developed to examine the performance of a wave energy focusing structure in combined waves and a current. With the current assumed to be slow and the structure fully submerged, the wave-current interaction problem can be reduced to a linear wave diffraction problem in a uniform surface current. The diffraction of regular incident waves around a submerged narrow structure of the shape of a parabola is considered. The energy focus is achieved by reflecting the incident waves through a predetermined focal point. Through numerical simulations, the numerical model is shown to be effective in modeling the wave-current interaction problem, and the current speed and direction are shown to affect significantly the location, amplitude and sharpness of the focus.

### INTRODUCTION

The enormous potential of ocean wave energy has prompted many studies to investigate the technical and economic feasibility of wave energy extraction. In particular, wave energy focusing structures have been proposed to amplify the incident wave height at a predetermined focal point, where the converged wave energy is harnessed by means of a mechanical power generator. A number of studies have been performed on various wave focusing devices to investigate their performance under different wave conditions.

A horizontal thin plate submerged under the free surface was proposed by Helstad (1980). The concept was further examined numerically and experimentally by Kudo et al. (1987), Imai et al. (1988) and Murashige and Kinoshita (1992) using thin plates of different shapes and dimensions. The use of lens-shaped vertical structures on the seabed has been examined by Mehlum and Stamnes (1980) and McCormick et al. (1980). Ertekin and Monopolis (1985) investigated the use of a parabolic step for wave energy focusing through a series of experiments and later studied the problem numerically (Yang and Ertekin, 1990). Gug and Lee (1992) considered the use of submerged structures on the seabed and the convergence of wave energy is achieved by refracting the incident plane waves over the gentle side slopes of the structure.

A different type of wave focusing structure is considered here, in which the wave energy is reflected by a submerged narrow structure on the seabed through a predetermined focal point. The centerline of the structure is defined by a parabola, similar to that of an optical reflector. The dimensions of the structure considered here are much smaller than those examined by Mehlum and Stamnes (1980), McCormick et al. (1980) and Gug and Lee (1992), and the focal point is located in front of the structure.

However, the work of Cheung et al. (1995) on wave-current interaction has shown that the presence of a current would modify significantly the diffracted wave field and amplitude near the structure. Accurate predictions of the performance of this wave focusing structure in combined waves and currents are therefore important in its design and operation in a coastal environment.

An approach to treat the wave-current interaction problem is to separate the flow field into a steady component associated with the current and a propagating component associated with the waves. With the assumption of a slow current, the free surface boundary conditions for the steady current component can be reduced to a rigid-wall condition, while the linear free surface boundary conditions for the propagating wave component are extended to include the modified current field. Based on this approach, Isaacson and Cheung (1993) and Cheung et al. (1995) provided a time-domain solution for the two- and three-dimensional problems, respectively. Comparisons of the numerical models have been made with the frequency domain solutions of Zhao and Falinsen (1988) and Nossen et al. (1991), and indicate favorable agreement.

The numerical model of Cheung et al. (1995) deals with the effects of a collinear current on the diffraction of regular waves around a three-dimensional surface piercing structure. The structure considered here is fully submerged, and the wave-current interaction problem can be simplified and reduced to a wave diffraction problem in a uniform surface current. The numerical model is extended to include effects of oblique incident waves and a current. The performance of the wave focusing structure in combined waves and a current is investigated. Emphasis is placed on the relations between the location, amplitude and sharpness of the focus, and the current speed and direction.

### THEORETICAL FORMULATION

#### Problem Statement

With reference to Fig. 1, the boundary-value problem is defined with a right-handed Cartesian coordinate system ( $x, y, z$ ), in which  $x$  and  $y$  are measured horizontally and  $z$  is measured vertically upwards from the still water level. The water depth in the computational domain is constant and is denoted by  $d$ . A sub-

Received February 25, 1995; revised manuscript received by the editors August 17, 1995. The original version (prior to the final revised manuscript) was presented at the Fifth International Offshore and Polar Engineering Conference (ISOPE-95), The Hague, The Netherlands, June 11-16, 1995.

KEY WORDS: Current, diffraction, reflection, wave energy, wave energy focusing, waves.

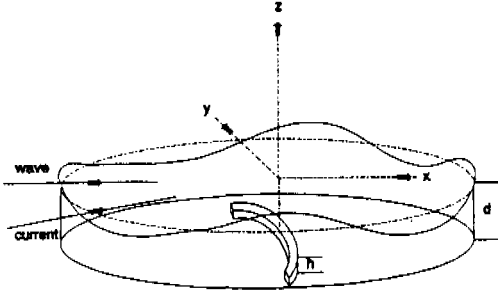


Fig. 1 Definition sketch

merged structure with a constant height  $h$  is located at the center of the domain. The incident waves are two-dimensional in the  $x$ - $z$  plane and progressive in the positive  $x$  direction. The direction of the uniform current is arbitrary and independent of the direction of the incident waves.

The fluid is assumed to be incompressible and inviscid, and the flow irrotational. The flow field is therefore described by a velocity potential  $\phi$  satisfying the Laplace equation:

$$\nabla^2 \phi = 0 \quad (1)$$

Since a linear solution is sought, the potential can be expressed as a sum of individual components proportional to the current speed and wave height, respectively:

$$\phi = U(x \cos \alpha + y \sin \alpha) + \phi_b + \phi_w + \phi_s \quad (2)$$

where  $U$  is the current speed and  $\alpha$  is the direction of the uniform current with respect to the positive  $x$ -axis. The first term on the right-hand side of Eq. 2 corresponds to the potential of the uniform current;  $\phi_b$  is the steady disturbance to the uniform current due to the presence of the structure; and  $\phi_w$  and  $\phi_s$  indicate respectively the incident and scattered wave components. Since the current speed is assumed to be small, the steady component of the free surface elevation associated with the current is negligible. The free surface elevation is simply expressed as a sum of the incident and scattered wave components as:

$$\eta = \eta_w + \eta_s \quad (3)$$

For the case of regular incident waves riding on a uniform current, linear wave theory gives respectively the incident potential and free surface elevation as:

$$\phi_w = \frac{\pi H}{kT} \frac{\cosh[k(z+d)]}{\sinh(kd)} \sin(kx - \omega_c t) \quad (4)$$

$$\eta_w = \frac{H}{2} \cos(kx - \omega_c t) \quad (5)$$

where  $H$  is the incident wave height;  $T$  is the wave period relative to the uniform current;  $k$  is the wave number;  $\omega_c = \omega + kU \cos \alpha$  is the angular frequency of the incident waves relative to a fixed reference frame; and  $\omega = 2\pi/T$  is the angular frequency relative to the uniform current.

### Boundary-Value Problem

The boundary-value problem for the scattered potential is defined here. The boundary conditions on the seabed and structure surface  $S_s$  are given respectively by:

$$\frac{\partial \phi_s}{\partial z} = 0 \quad \text{at } z = -d \quad (6)$$

$$\frac{\partial \phi_s}{\partial n} = -\frac{\partial \phi_w}{\partial n} \quad \text{on } S_s \quad (7)$$

where  $n$  is distance in the direction of the normal. Due to the presence of the current, the kinematic and dynamic free surface boundary conditions are modified respectively to:

$$\begin{aligned} \frac{\partial \phi_s}{\partial z} - \frac{\partial \eta_s}{\partial t} - U \left( \frac{\partial \eta_s}{\partial x} \cos \alpha + \frac{\partial \eta_s}{\partial y} \sin \alpha \right) &= \left( \frac{\partial \eta_w}{\partial x} + \frac{\partial \eta_s}{\partial x} \right) \frac{\partial \phi_b}{\partial x} \\ &+ \left( \frac{\partial \eta_w}{\partial y} + \frac{\partial \eta_s}{\partial y} \right) \frac{\partial \phi_b}{\partial y} - (\eta_w + \eta_s) \frac{\partial^2 \phi_b}{\partial x^2} \quad \text{on } S_o \end{aligned} \quad (8)$$

$$\begin{aligned} \frac{\partial \phi_s}{\partial t} + g \eta_s + U \left( \frac{\partial \phi_s}{\partial x} \cos \alpha + \frac{\partial \phi_s}{\partial y} \sin \alpha \right) &= - \left( \frac{\partial \phi_w}{\partial x} + \frac{\partial \phi_s}{\partial x} \right) \frac{\partial \phi_b}{\partial x} \\ &- \left( \frac{\partial \phi_w}{\partial y} + \frac{\partial \phi_s}{\partial y} \right) \frac{\partial \phi_b}{\partial y} \quad \text{on } S_o \end{aligned} \quad (9)$$

where  $S_o$  is the still water surface. The terms on the right-hand sides of Eqs. 8 and 9 account for the modifications of the incident and scattered waves by the local surface current near the structure. If the structure is fully submerged and its sectional dimensions are small compared with the water depth, the modification of the surface current near the structure is negligible. The terms on the right-hand sides are therefore small compared to the other terms and need not be considered. Consequently, the solution of  $\phi_b$  is not required and the computing time is reduced.

Due to the presence of the current, the celerity of the scattered waves varies depending on the directions of the waves and the current. The radiation condition is extended to account for the spatially dependent celerity on the control surface:

$$\frac{\partial \phi_s}{\partial t} + c \frac{\partial \phi_s}{\partial n} = 0 \quad (10)$$

where  $c$  is the locally determined celerity of the outgoing waves on the control surface (Isaacson and Cheung, 1992.)

The solution to the boundary-value problem of the scattered potential may be obtained by the application of an integral equation involving a Green function  $G$ :

$$\phi_s(\mathbf{x}) = \frac{1}{2\pi} \int_S \left[ G(\mathbf{x}, \boldsymbol{\xi}) \frac{\partial \phi_s}{\partial n} - \phi_s(\mathbf{x}) \frac{\partial G}{\partial n}(\mathbf{x}, \boldsymbol{\xi}) \right] dS \quad (11)$$

Here  $\boldsymbol{\xi}$  represents a point  $(\xi, \psi, \zeta)$  on the surface  $S$  over which the integration is performed and  $n$  is measured from the point  $\boldsymbol{\xi}$ . The surface  $S$  would comprise the structure surface, the still water surface, the seabed and a control surface truncating the infinite fluid region. With the seabed horizontal, it is more efficient to exclude the seabed from  $S$  and to choose a Green function that accounts for the symmetry about the seabed. This is:

$$G(\mathbf{x}, \xi) = \frac{1}{|\xi - \mathbf{x}|} + \frac{1}{|\xi' - \mathbf{x}|} \quad (12)$$

The source point  $\xi' = [\xi, \psi, -(\zeta + 2d)]$  is the image of  $\xi$  about the seabed. If the flow field is also symmetric about the  $x$  axis, the Green function that accounts for double symmetry can be used instead (e.g. Cheung et al., 1995).

### Summary of Numerical Procedures

The numerical procedure described in Isaacson and Cheung (1992, 1993) can be applied to the above formulation and only a brief summary is provided here. The solution to the boundary-value problem is obtained by a numerical discretization, in which the surfaces are discretized into finite numbers of planar quadrilateral facets. The values of  $\phi_s$  and  $\partial\phi_s/\partial n$  are taken as constant over each facet and applied at the centroid. The integral equation is then reduced to a system of simultaneous equations. Since the coefficients of the equations are functions of the geometry and discretization only, the solution to the system of equations is required only once and the numerical model can be applied to different incident wave and current conditions.

The input vector to the system of equations consists of the normal derivative of the scattered potential on the structure surface, which is known from the body surface boundary condition, as well as the potential on the control surface and the still water surface, which may be obtained by a time-stepping procedure applied to the corresponding boundary conditions. Initial conditions at  $t = 0$  correspond to an undisturbed regular wave train and a uniform current in the computational domain. The value of the scattered wave potential is zero and the structure has no effects on the flow. The body surface boundary condition is imposed gradually over the first wave cycle through the use of a modulation function, and a steady state solution in the vicinity of the structure is usually developed after the first cycle.

### RESULTS AND DISCUSSION

To illustrate the numerical model and to examine the proposed wave energy focusing structure, the diffraction of regular incident waves in a uniform current around a submerged narrow structure on the seabed is considered. The centerline of the structure is defined by the parabola  $y^2 = -4ax$ , where the vertex of the parabola is located at the origin of the  $x$  and  $y$  axes as shown in Fig. 1, and the constant  $a$  is the distance between the focal point and the vertex. In the numerical example considered here, the width and length of the structure and the theoretical location of the focal point are, respectively,  $0.16L$ ,  $2L$  and  $1.27L$ , where  $L$  is the incident wavelength. The water depth corresponds to  $kd = 0.5$ , and the height of the structure is equal to one-half of the water depth ( $h/d = 0.5$ ). The dimensions of the computational domain are  $3L \times 3L$ .

As a benchmark for comparison, a special case when the current speed is equal to zero is considered first. Fig. 2 shows the perspective view and contour plots of the wave amplitude over the computational domain. The wave amplitude in the contour plots is normalized by the incident wave amplitude, and the normalized amplitude at the focal point represents the amplification factor. The outline of the energy focusing structure is also shown along with the contour plots. The structure functions like an optical reflector and the reflected waves converge near the predetermined focal point, forming a system of partial standing waves with a series of peaks. The wave amplitude behind the structure is not affected significantly. The maximum peak is  $1.16L$  from

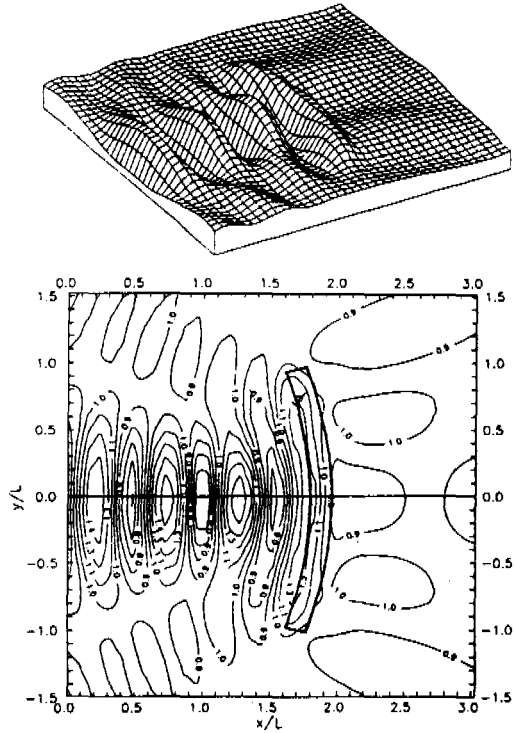


Fig. 2 Perspective view and contour plots of computed wave amplitude for  $U/\sqrt{gd} = 0$

the center of the structure and the amplification factor is 1.53. Since the wave energy is proportional to the square of the wave height, this represents more than a 230% increase in energy level. Further increase in energy level is possible by adjusting the height, length and curvature of the structure.

When the incident waves and the current are collinear, Figs. 3 and 4 show the computed wave amplitudes for  $\alpha = 0^\circ$  and  $180^\circ$ , respectively. The current speed for both cases is identical and is specified in terms of the Froude number,  $U/\sqrt{gd} = 0.2$ . For  $\alpha = 0^\circ$ , the incident waves and the current are in the same direction and the reflected waves from the structure propagate against the current, giving rise to shorter wavelengths and higher amplitudes. As shown in Fig. 3, the partial standing wave system formed in the vicinity of the structure is modified significantly by the current. The focal point is shifted toward the structure and both the sharpness and amplitude of the focus increase. For  $\alpha = 180^\circ$ , the incident waves and the current are in the opposite directions and the reflected waves propagate with the current, giving rise to longer wavelengths and lower wave amplitudes. As shown in Fig. 4, the focal point is shifted toward the structure and both the sharpness and amplitude of the focus decrease.

Figs. 5 and 6 show the computed wave amplitudes for  $\alpha = 45^\circ$  and  $90^\circ$ , respectively. The Froude number is identical in both cases and equal to 0.2. For  $\alpha = 45^\circ$ , the component of the current velocity in the  $x$  direction causes the formation of higher and shorter reflected waves, while the  $y$  component of the current deflects the direction of the reflected waves. The focal point is shifted in the direction of the current, while an increase in ampli-

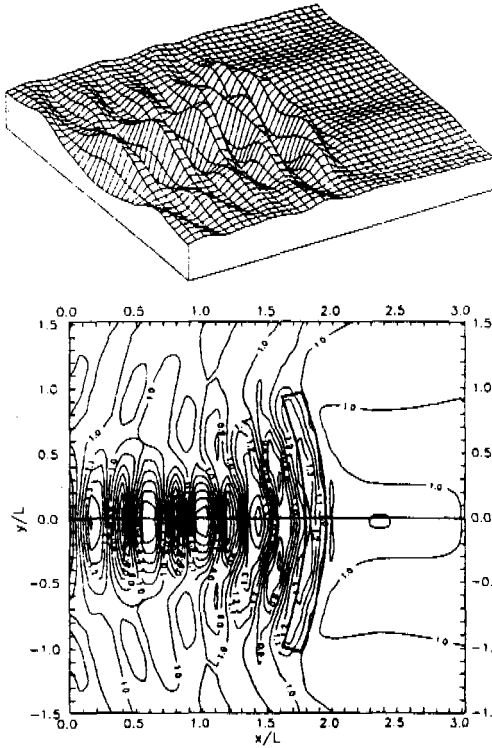


Fig. 3 Perspective view and contour plots of computed wave amplitude for  $U/\sqrt{gd} = 0.2$  and  $\alpha = 0^\circ$

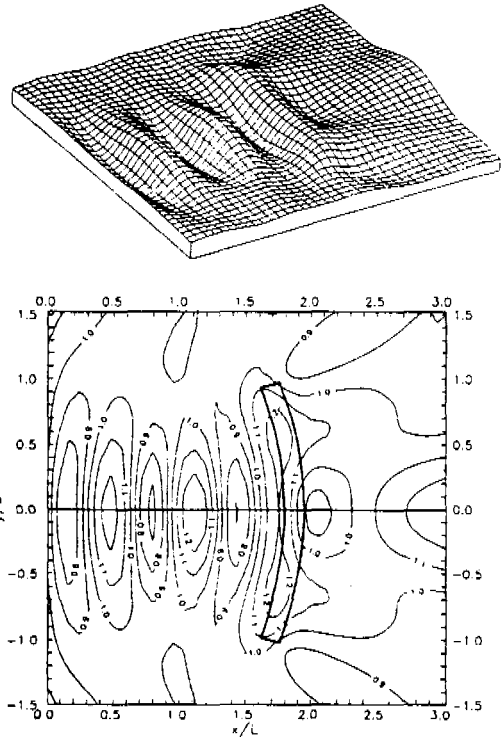


Fig. 4 Perspective view and contour plots of computed wave amplitude for  $U/\sqrt{gd} = 0.2$  and  $\alpha = 180^\circ$

amplitude is observed. When the current is in the  $y$  direction perpendicular to the incident waves, the amplitude and phase of the wave profile in the  $x$  direction are not significantly affected, while the general pattern of the wave amplitude is shifted in the direction of the current as shown in Fig. 6.

Of particular interest is the modification of the amplification factor by the current. Fig. 7 shows the amplification factor as a function of the Froude number and current direction. For  $\alpha = 0^\circ$ , the amplification factor increases initially with the Froude number due to the formation of higher reflected waves. At higher values of the Froude number, the amplification factor stabilizes and then decreases, since the increase in the reflected wave height is offset by the phase shift between the incident and reflected waves. Similarly, the amplification factor for  $\alpha = 45^\circ$  is expected to stabilize for higher values of the Froude number. For  $\alpha = 90^\circ$ , the wave pattern is shifted in the  $y$  direction and the amplification factor remains relatively constant within the range of Froude number considered. When the waves and the current are in opposite directions, the amplification factor decreases with the Froude number due to lower and longer reflected waves.

The shift of the focal point in the presence of a current is important in the positioning of the wave power generator. Figs. 8a and 8b show respectively the displacements of the focal point in the  $x$  and  $y$  directions as functions of the Froude number and current direction. The displacements are calculated with respect to the predetermined location of the focal point, when there is no current. The displacement of the focal point in the  $x$  direction is due to the modification of the wavelength and amplitude of the

reflected waves, while the displacement in the  $y$  direction is a result of the current component in that direction. Therefore, no displacement of the focal point in the  $x$  direction is observed when  $\alpha = 90^\circ$ , and no displacement in the  $y$  direction is observed when  $\alpha = 0$  and  $180^\circ$ . For  $\alpha = 45^\circ$  and  $90^\circ$ , the displacement of the focal point in the  $y$  direction increases linearly with the Froude number. For the conditions considered here, the displacement of the focal point may span a significant fraction of a wavelength.

## CONCLUSIONS

The performance of a wave focusing structure in combined waves and a current has been examined by a time-domain method. The dimensions of the proposed structure are an order of magnitude smaller than those of conventional wave focusing structures, and the wave energy focus is formed by diffracting and reflecting the incident waves. To illustrate the numerical model, a submerged narrow structure on the seabed is examined. The centerline of the structure is defined by a parabola with a predetermined focal point. The wave amplitude profile, amplification factor and displacement of the focal point are presented as functions of the Froude number and current direction.

The numerical model has been shown capable of simulating the various wave-current interaction mechanisms. Through the numerical simulations, the proposed structure is shown to be effective in focusing the incident wave energy. The simulations indicate that the energy density increases not only at the focal

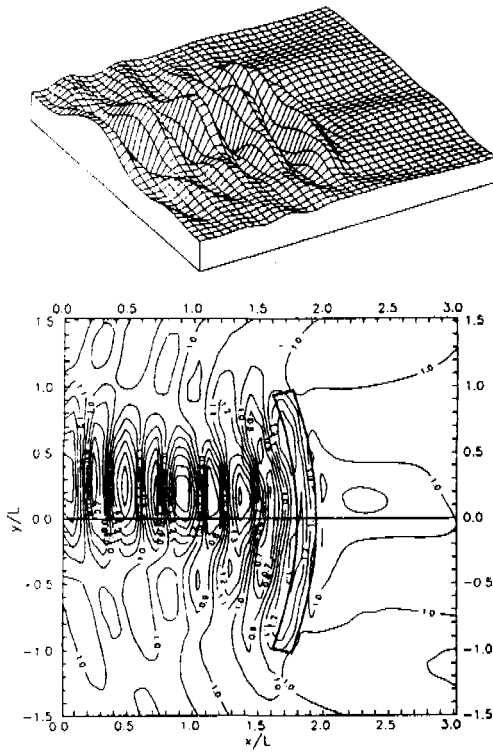


Fig. 5 Perspective view and contour plots of computed wave amplitude for  $U/\sqrt{gd} = 0.2$  and  $\alpha = 45^\circ$

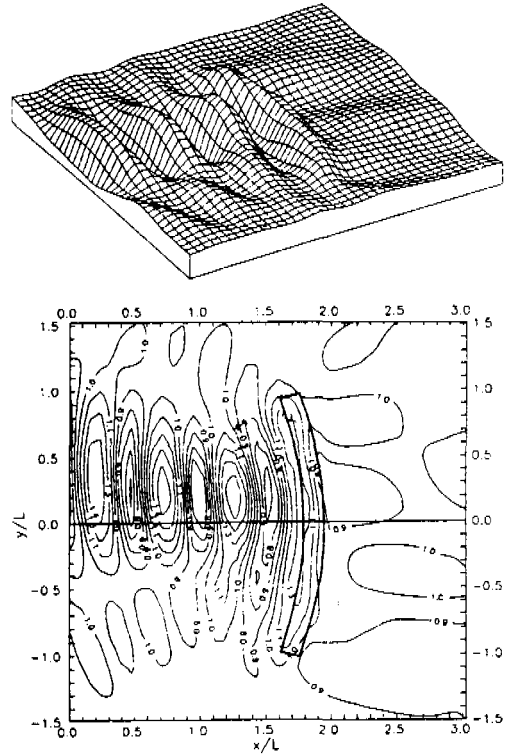


Fig. 6 Perspective view and contour plots of computed wave amplitude for  $U/\sqrt{gd} = 0.2$  and  $\alpha = 90^\circ$

point, but also at a series of locations in front of the structure. The results also illustrate the importance of a current on the performance of the structure. Depending on the current speed and direction, the amplitude and location of the focus might be modified significantly. The effects of a current should be considered in the design and operation of this type of wave energy focusing structure.

ACKNOWLEDGMENTS

This study was supported by the Academic Research and Promotion Division, Ministry of Education, Korea, and was carried out when the second author was a visiting professor at the University of Hawaii at Manoa in 1994. SOEST Contribution No. 3904.

REFERENCES

Cheung, KF, Lee, JW, and Isaacson, M (1995). "Wave Diffraction Around a Three-Dimensional Body in a Current." *Proc Conf Offshore Mech and Arctic Eng*, Copenhagen, Vol 1A, pp 395-402.  
 Ertekin, RC, and Monopolis, GM (1985). "Investigation of Wave Focusing over a Parabolic Step," *Hydro Ocean Wave-Energy Utilization*, ed DV Evans and AF de O Falcao, pp 433-346.  
 Gug, SG, and Lee, JW (1992). "A Study on the Concentration of Wave Energy by Construction of a Submerged Coastal Structure," *J Korean Inst Port Res*, Vol 6, No 1, pp 35-51.  
 Helstad, J (1980). "Power Production Based on Focused Ocean Swell,"

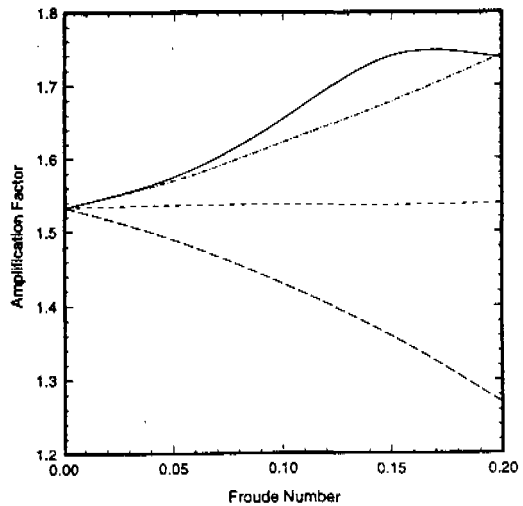


Fig. 7 Amplification factor as a function of Froude number and current direction. —,  $\alpha = 0^\circ$ ; - - - -,  $\alpha = 45^\circ$ ; - · - ·,  $\alpha = 90^\circ$ ; - - - -,  $\alpha = 180^\circ$

*Norwegian Maritime Res*, Vol 4, pp 34-42.  
 Imai, K, Akiyama, Y, and Kudo, K (1988). "Wave Focusing Due to a

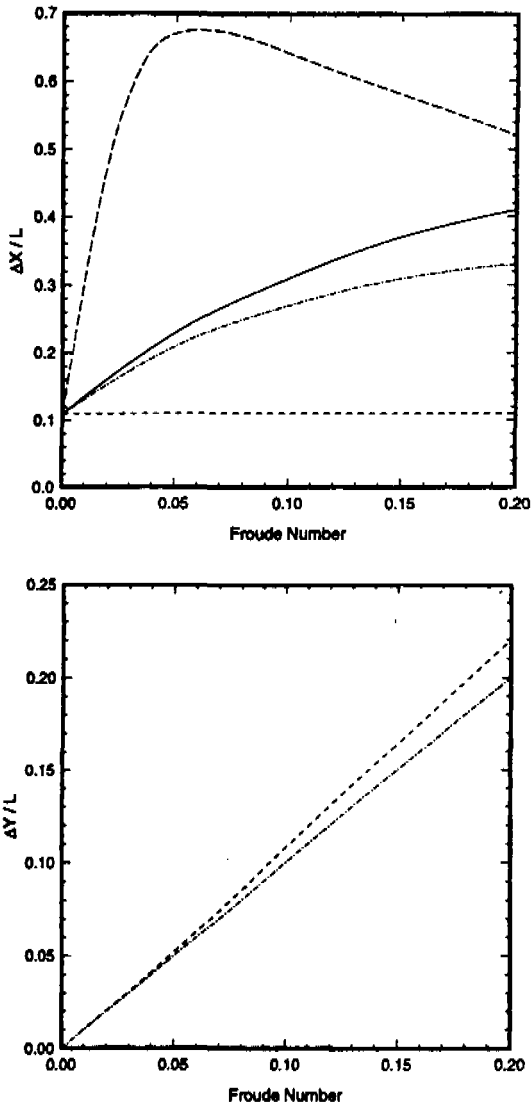


Fig. 8 Displacement of focal point as a function of the Froude number and current direction. (a) x direction. (b) y direction. —,  $\alpha = 0^\circ$ ; ·····,  $\alpha = 45^\circ$ ; - · - ·,  $\alpha = 90^\circ$ ; - - -,  $\alpha = 180^\circ$ .

Submerged Crescent Plate," *Coastal Eng Japan*, Vol 31, No 2, pp 231-243.

Isaacson, M, and Cheung, KF (1992) "Time-Domain Second-Order Wave Diffraction in Three Dimensions," *J Waterway, Port, Coastal & Ocean Eng*, Vol 118, No 5, pp 496-516.

Isaacson, M, and Cheung, KF (1993). "Time-Domain Solution for Wave-Current Interactions with a Two-Dimensional Body," *Applied Ocean Res*, Vol 15, No 1, pp 39-52.

Kudo, K, Tsuzuku, T, Imai, K, and Akiyama, Y (1987). "A Wave Focusing Phenomenon by a Submerged Plate," *J Soc of Naval Arch Japan*, Vol 106, pp 35-43

McCormick, M, Kastner, R, and Glover, L (1980). "Water Wave Focusing by Submerged Lens-Shaped Structures," U.S. Naval Acad, Rept EW-14-80.

Mehlum, E, and Stamnes, J (1980). "On the Focusing of Ocean Swells and Its Significance in Power Production," *Proc 1st Symp Wave Energy Utilization*, Gothenburg, Sweden, pp 29-35.

Murashige, S, and Kinoshita, T (1992). "An Ideal Ocean Wave Focusing Lens and its Shape," *Applied Ocean Res*, Vol 14, No 4, pp 275-290.

Nossen, J, Grue, J, and Palm, E (1991). "Wave Forces on Three-Dimensional Floating Bodies with Small Forward Speed," *J Fluid Mech*, Vol 227, pp 135-160.

Yang, C, and Ertekin, RC (1990). "Numerical Simulation of Wave-Energy Focusing," *Proc Oceans 91*, Honolulu, Vol 1, pp 539-546.

Zhao, R, and Faltinsen, OM (1988). "Interaction Between Waves and Current on a Two-Dimensional Body in the Free Surface," *Applied Ocean Res*, Vol 10, No 2, pp 87-99.